Published in final edited form as:
*J Comp Pathol*. 2013 November ; 149(4): 434–445. doi:10.1016/j.jcpa.2013.03.008.

# Immunohistochemical Characterization of the Hepatic Progenitor Cell Compartment in Medaka (*Oryzias latipes*) following Hepatic Injury

**A. J. Van Wettere**[*,†], **S. W. Kullman**[†,‡], **D. E. Hinton**[§], and **M. Law**[*,†]

[*]Department of Population Health and Pathobiology, North Carolina State University, Raleigh, North Carolina, USA

[†]Center for Comparative Medicine and Translational Research, North Carolina State University, Raleigh, North Carolina, USA

[‡]Department of Environmental and Molecular Toxicology, North Carolina State University, Raleigh, North Carolina, USA

[§]Nicholas School of the Environment, Duke University, Durham, North Carolina, USA

## Summary

Laboratory fish species are used increasingly in biomedical research and are considered robust models for the study of regenerative processes. Studies investigating the response of the fish liver to injury have demonstrated the presence of a ductular reaction and oval-like cells in injured and regenerating liver. To date, however, it is unclear if this cell population is the piscine equivalent of oval cells or intermediate hepatobiliary cells identified in rodents and man, respectively. The present study defines the process of oval cell differentiation in fish liver using histopathology, immunohistochemistry and transmission electron microscopy. To generate oval cell proliferation in Japanese medaka (*Oryzias latipes*), hepatic injury was induced by exposure of adult fish to either microcystin LR or dimethylnitrosamine. A transgenic strain of medaka expressing a red fluorescent protein (RFP) exclusively in hepatocytes was used. The morphological response to injury was characterized by a ductular reaction comprised of cytokeratin (CK) AE1/AE3$^{+}$ oval cells progressing to intermediate hepatobiliary cells variably positive for CK and RFP, and finally mature RFP$^{+}$ hepatocytes and CK$^{+}$ cholangiocytes. These observations support a bipotential differentiation pathway of fish oval cells towards hepatocytes and cholangiocytes. Ultrastructural morphology confirmed the presence of oval cells and differentiation towards hepatocytes. These results demonstrated clear similarities between patterns of reaction to injury in fish and mammalian livers. They also confirm the presence of and support the putative bipotential lineage capabilities of the fish oval cell.

Correspondence to: A. Van Wettere, (van_wetterea@hotmail.com).

**Conflict of Interest Statement**

The authors declared no potential conflicts of interest with respect to the research, authorship and/or publication of this article.

**Keywords**

fish; liver; bile preductular epithelial cell; oval cell

## Introduction

Laboratory fish species are used increasingly in biomedical research and are considered robust models for the study of regenerative processes in organs such as the fin and heart; however, the process of hepatic regeneration in fish has received less attention (Poss, 2007; Sadler *et al*., 2007; Kan *et al*., 2009; Cheng *et al*., 2012). Studies have demonstrated that the hepatic regenerative response (compensatory growth) in fish is comparable with those of rodents and man (Okihiro and Hinton, 2000; Sadler *et al*., 2007; Kan *et al*., 2009; Hobbie *et al*., 2011). Following partial hepatectomy, compensatory liver growth in zebrafish (*Danio rerio*) and rainbow trout (*Oncorhynchus mykiss*) occurs via proliferation of mature hepatocytes (zebrafish) or a combination of hepatocytes and cells that are presumed to be derived from hepatic progenitor cells (HPCs) due to their morphological resemblance to rodent oval cells (rainbow trout) (Okihiro and Hinton, 2000; Sadler *et al*., 2007; Kan *et al*., 2009). In studies evaluating the hepatic response to toxic injury and hepatocarcinogenesis in fish species, proliferation of cells resembling rodent oval cells has been documented, and their presumptive differentiation towards hepatocytes inferred (Couch and Courtney, 1987; Hinton *et al*., 1988; Nunez *et al*., 1990; Okihiro and Hinton, 2000; Fournie and Courtney, 2002; Hobbie *et al*., 2011). Although the fish liver reaction to injury appears similar to that of mammals, it has not known whether the oval-like cells observed in the fish liver are the biological equivalent of rodent oval cells and human intermediate hepatobiliary cells (IHBCs).

In mammals, liver regeneration after injury is accomplished primarily through proliferation of mature hepatocytes (Riehle *et al*., 2011); however after severe hepatic injury or when hepatocyte division is impaired, HPCs participate in the regenerative process and are the alleged precursor cells of hepatocytes and cholangiocytes (Evarts *et al*., 1989; Fausto and Campbell, 2003; Riehle *et al*., 2011). These HPCs are also a possible cell of origin of hepatic tumours, further stressing the importance of understanding their biology (Mikhail and He, 2011). A third pathway of liver regeneration by fusion or transdifferentiation of bone marrow stem cells into hepatocytes has been documented, although this pathway is not considered clinically significant (Oh *et al*., 2007; Riehle *et al*., 2011).

Previous studies examining normal fish hepatic histology described a population of small cholangiocytes with high nuclear to cytoplasmic ratio that was termed ‘bile preductular epithelial cells’ (BPDECs) (Okihiro and Hinton, 2000; Fournie and Courtney, 2002; Hinton *et al*., 2008; Hobbie *et al*., 2011). The fish liver has numerous ‘bile preductules’ that are transition canals between the biliary canaliculi formed by adjacent hepatocytes and the bile ductules which are entirely lined by biliary epithelial cells (Hardman *et al*., 2007). Bile preductules are formed by BPDECs and hepatocytes. Hence, BPDECs reside in a location equivalent to mammalian cholangiocytes in the canal of Hering (Hardman *et al*., 2007). In mammals, the small cholangiocytes located in the canal of Hering are believed to be

facultative HPCs (Fausto and Campbell, 2003; Roskams *et al*., 2004; Desmet, 2011). It should be noted that the terminology used in the literature to describe HPCs and their resultant transient amplifying cell population in histology sections can be confusing. In man, cholangiocytes in the canal of Hering/HPCs and IHBCs observed in the ductular reaction are considered the equivalent of oval cells in rodents (Roskams *et al*., 2004). The descriptive term ‘oval cell’ is discouraged because rodent oval cells are not considered comparable with their human equivalent (Roskams *et al*., 2004). In fish, the proliferating cell population observed after hepatic injury, resembling oval cell hyperplasia in rodents, has been described as BPDECs hyperplasia (Okihiro and Hinton, 2000; Hinton *et al*., 2008; Hobbie *et al*., 2011).

In addition to sharing a common location, fish ‘BPDECs’, rodent ‘oval cells’ and human ‘HPCs’ each share common ultrastructural morphology, thus further supporting their probable equivalence (Factor *et al*., 1994; Hardman *et al*., 2007; Sobaniec-Lotowska *et al*., 2007). Moreover, in trout primary liver cultures, the longest living cells shared morphological features and immunoreactivity (expressing cytokeratin [CK] AE1/AE3) with BPDECs (Ostrander *et al*., 1995). Since this longevity is evocative of a ‘stem cell-like’ state, this further supports the hypothesis that BPDECs are the HPC in fish.

In the present study we hypothesized that the oval cells observed in injured medaka liver are a transient amplifying cell population derived from progenitor cells and have bipotential differentiation into hepatocyte and biliary cell lineages. The aim of the study was to determine the immunohistochemical and ultrastructural characteristics of the putative piscine progenitor cell compartment after acute and chronic hepatic injury.

## Materials and Methods

### Fish

A transgenic orange-red medaka fish line Tg(zfL-fabp:DsRed), which express a red fluorescent protein (RFP) under the regulatory control of the 2.8 kb fragment of the zebrafish liver fatty acid binding protein promoter (Korzh *et al*., 2008), was used. The Tg(zfL-fabp:DsRed) medaka stock colony was housed under recirculating freshwater aquaculture conditions at the Department of Molecular and Environmental Toxicology, North Carolina State University, Raleigh, North Carolina.

### Dimethylnitrosamine and Microcystin LR Exposure

Three-month-old male and female medaka from the stock colony were acclimatized for 2 weeks in a 40 l aquarium filled with reconstituted reverse osmosis–purified water (0.5 g/l Instant Ocean® salts, Aquarium Systems Inc., Mentor, Ohio, USA) within a static, freshwater culture system. The artificial photoperiod was 16 h light/8 h dark. The water temperature was maintained at 26 ± 0.5°C, the water pH at 6.5 ± 0.5 and the water conductivity between 600 to 800 μS. Dry food (Otohime B1, Reed Mariculture, Campbell, California, USA) was fed five times per day using automated feeders. Animal care and use followed protocols approved by the North Carolina State University Animal Care and Use Committee in accordance with the National Academy of Sciences Guide for the Care and

Use of Laboratory Animals. For the dimethylnitrosamine (DMN) and micocystin LR (MCLR) exposures, medaka were distributed randomly in groups of 10–12 randomly between 4 l glass beakers containing 3 l of reconstituted water. The beakers were placed within a recirculating, heated water bath to maintain temperature at 26 ± 0.5°C throughout the exposures. Fish were fed once daily.

### Microcystin LR Exposure

These fish were part of MCLR dose range-finding exposures. Doses were extrapolated from the literature (Malbrouck and Kestemont, 2006; Djediat *et al*., 2010). In total, 21, 27 and 12 Tg(zfL-fabp:DsRed) medaka received a single intracoelomic injection of MCLR of 100, 250 and 500 ± 25 μg/kg, respectively. The MCLR stock solution was dissolved in sterile phosphate buffered saline (PBS; pH 7.2) at a concentration of 0.025 μg/μl. Fish were briefly anaesthetized using buffered tricaine methanesulphonate (120 mg/l; MS-222, Argent Laboratories, Redmond, Washington, USA), weighed, placed in right lateral recumbency, and injected intraperitoneally using a glass 25 μl Hamilton syringe (PB-600 Repeating Dispenser, Hamilton, Reno, Nevada, USA), equipped with a 32 gauge needle. Twenty control fish were anaesthetized and injected with 4 μl of sterile PBS. A subset of at least two MCLR-exposed and one control medaka were killed with an overdose of tricaine methanesulphonate (300 mg/l) at 1, 2, 4, 6 or 8 days post exposure for histology. The coelom of control and exposed fish was incised along the ventral midline to enhance penetration of the fixative. The fish were fixed whole in 4% paraformaldehyde solution for 24 h, demineralized in 10% formic acid for 24 h and transferred to 70% ethanol for histology.

### Dimethylnitrosamine Exposure

Eighteen Tg(zfL-fabp:DsRed) medaka were exposed to 100 μg/l (ppm) of DMN for 2 weeks in the ambient water. Nine fish were used as controls. The DMN exposure dose was based on a previous study (Van Wettere *et al*., 2012). DMN was replaced every 3 days to compensate for photodegradation of the compound (Hobbie *et al*., 2011). DMN dilutions were made freshly from the DMN stock solution before each renewal. Water quality was maintained with change of 95% of the water prior to each DMN treatment. Ammonia levels remained under 0.25 mg/l at all times. After the 2-week exposures, fish were returned to the 40 l aquarium tanks for up to 8 weeks. Six DMN-exposed and three control fish were killed with an overdose of tricaine methanesulphonate (300 mg/l) at 4, 6 or 8 weeks post exposure. Individual fish livers were harvested and fixed for 24 h in 4% paraformaldehyde solution for histopathology. Samples of each liver were also fixed in 4F:1G fixative (4% formaldehyde and 1% glutaraldehyde buffered in monobasic sodium phosphate, pH 7.2) for transmission electron microscopy (TEM) (McDowell and Trump, 1976).

### Histopathology

Fixed livers and whole fish were processed routinely and sections were stained with haematoxylin and eosin (HE). Liver lesions were classified based on criteria set by a consensus of the US National Toxicology Program Pathology Working Group and the guide to international harmonization of nomenclature and diagnostic criteria for lesions in rats and

mice (Boorman et *al*., 1997; Thoolen *et al*., 2010). In the present study, the descriptive terms 'oval cell' and 'oval cell hyperplasia' were applied. Although fish oval cells might be derived from BPDECs and the term 'BPDEC hyperplasia' has been used in other studies, we reserved the term 'oval cell' for the transient amplifying population that resemble rodent oval cells and the term BPDECs for the quiescent cholangiocytes in the bile preductules. Medaka oval cells were defined by histological or TEM phenotype and were immunoreactive for CK only. Oval cells were elongated to round cells with a high nuclear to cytoplasmic ratio and round to oval hyperchromatic nuclei that were often organized in a single or double row in linear arrays and pseudoduct-like structures (Figs. 1 and 3) resembling a 'ductular reaction' in human liver and 'oval cell hyperplasia' in rodent liver (Roskams *et al*., 2004; Thoolen *et al*., 2010). Medaka IHBCs were defined as cells with an intermediate histological or TEM phenotype between oval cells and hepatocytes or cholangiocytes, and immunoreactivity for CK and RFP.

### Transmission Electron Microscopy

Liver samples were processed routinely for TEM (Dykstra, 1993). Ultrathin sections were stained with uranyl acetate and lead citrate and examined with a FEI/Philips EM 208S transmission electron microscope (Laboratory for Advanced Electron and Light Optical Methods, North Carolina State University).

### Immunohistochemistry

Sections of fixed medaka livers were used for single and double immunohistochemistry (IHC). Primary antibodies against CK AE1/AE3, muscle-specific actin (MSA), RFP and proliferating cell nuclear antigen (PCNA) were used (Table 1). For antigen retrieval the slides were heated at 99°C in a 10 mM sodium citrate solution (pH 6.0) for 10 min using a vegetable steamer (Oster 5712 food steamer, Maitland, Florida, USA). For single IHC, the Biogenex SuperSensitive Link-Label IHC Detection System (BioGenex San Ramon, California, USA) was used and labelling was 'visualized' using 3, 3′-diaminobenzidine (DAB, Vector Laboratories, Burlingame, California, USA) or NovaRED (Vector Laboratories). For double IHC, tissues were incubated with a primary antibody cocktail comprising reagents specific for CK and RFP, MSA and RFP, or CK and MSA, at room temperature for 30 min. The Thermo Fisher Scientific MultiVision Polymer Detection System (Thermo Fisher Scientific, Lab Vision Corporation, Fremont, California, USA) was used for detection and development was achieved using 3, 3′-diaminobenzidine (Vector Laboratories) followed by NovaRED (Vector Laboratories). Slides were counterstained with Mayer's haematoxylin. For negative controls, the primary antibody was omitted and non-immune serum of the same species as the primary antibody was applied. For positive controls, sections of medaka intestine and liver were included on each slide.

## Results

### Histopathology and Immunohistochemistry: MCLR Exposure

Hepatic necrosis with evidence of hepatic regeneration was observed in four of 21 (19%), five of 27 (19%) and three of 12 (25%) fish exposed to 100, 250 or 500 ± 25 μg/kg of MCLR, respectively (Table 2). In the fish that developed hepatic changes, the reaction to

injury was similar in character and time, and independent of the MCLR dose administered. Diffuse massive coagulative hepatocellular necrosis with few scattered clusters and short cords of polygonal basophilic cells were observed throughout the parenchyma at 14–36 h post exposure (Fig. 1). These cells were interpreted as proliferating oval cells. By 36–48 h post exposure, cords and tubules of basophilic cells were more numerous, longer, and started to merge with adjacent cords. Between the cords of regenerating cells, there were numerous macrophages that were filled with cell debris (Fig. 4). At 48–72 h post exposure, the number and size of the basophilic cells had increased further and the cells resembled IHBCs or small hepatocytes (Fig. 1). The number of macrophages had decreased (subjective assessment). At 96 h post exposure, the morphology and organization of the basophilic cells had progressed towards a hepatocyte phenotype with restoration of normal liver architecture (Fig. 1). The number of macrophages had decreased further. Mitotic figures were rare in the oval cells (< 1 per ×40 objective field). However, most oval cells at 24–96 h post exposure displayed strong nuclear immunoreactivity for PCNA, signifying that cell proliferation was occurring. No remarkable microscopical abnormalities were seen in the liver or other organs of the control animals.

At 24 and 48 h post exposure, the basophilic proliferating oval cells displayed strong diffuse cytoplasmic immunoreactivity for CK. Later, CK immunoreactivity subsided and was markedly decreased or absent by 96 h post exposure (Fig. 2). The oval cells were negative for RFP at 24 and 48 h post exposure. At 96 h post exposure, the liver of one of two fish exhibited mild to moderate immunoreactivity for RFP in IHBCs, while the other had rare IHBCs with faint cytoplasmic RFP immunoreactivity. Extracellular cell debris and the cytoplasm of macrophages were immunoreactive for RFP at 24 and 48 h post exposure, but immunoreactivity was weaker or absent at 96 h post exposure. Results of IHC are summarized in Table 3.

### Histopathology and Immunohistochemistry: DMN Exposure

The changes in the liver of DMN-exposed fish were similar to those described by Hobbie *et al*., (2011) and Van Wettere *et al*. (2012). Histological lesions included hepatocellular vacuolar degeneration, Mallory-Denk body-like inclusions, altered foci, necrosis, and collapse of the hepatic architecture, histiocytic inflammation, oval cell hyperplasia, hepatic stellate cell hyperplasia, biliary hyperplasia, fibrosis, hepatocellular regeneration and multinodular reorganization of the liver architecture. No remarkable microscopical abnormalities were seen in the liver of the control medaka other than occasional small areas of spongiosis hepatis in three of 9 (33%) controls (3/6 female and 0/3 male). Four of the 18 fish exposed to DMN (22%; three males and one female) exhibited prominent oval cell hyperplasia (Fig. 3). The remaining fish (67%; 10 females and two males) had moderate hepatic fibrosis. Two of the 12 (17%) fish, both female, had hepatic fibrosis with neoplasia; one hepatocellular carcinoma and one cholangiocellular carcinoma. Two fish (11%) died during the grow-out period; one of them was evaluated by histology and had severe hepatic fibrosis/cirrhosis. The other was autolyzed and was not evaluated.

The oval cell hyperplasia phenotype was characterized by diffuse loss of hepatocellular glycogen, scattered individual hepatocellular apoptosis or necrosis and marked proliferation

of elongated cells (oval cells) with oval hyperchromatic nuclei that extended along and sometimes surrounded hepatocytes. Hepatocytes were variably sized, often hypertrophic, with a variable degree of hydropic degeneration (hyalinization) (Fig. 3). In the fibrotic livers, deposition of collagenous extracellular matrix was mild to moderate, separated hepatocyte tubules and individualized single or small groups of hepatocytes. In livers with oval cell hyperplasia and to a lesser extent in the fibrotic livers, individualized or small groups of immature hepatocytes were observed (Fig. 3).

IHC revealed that the oval cells had intense, diffuse cytoplasmic expression of CK, but no labelling for RFP and MSA (Fig. 4). Intermediate hepatobiliary cells had variable cytoplasmic immunoreactivity for CK and RFP and were negative for MSA (Figs. 2 and 3). Double IHC for CK and RFP revealed occasional double labelling of the cytoplasm of IHBCs (Fig. 4). No cells demonstrated double labelling for CK and MSA or RFP and MSA. IHC for MSA showed cytoplasmic immunoreactivity in activated stellate cells present along sinusoids and in spindle cells surrounding mature bile ducts (Fig. 5). Similar MSA immunoreactivity was present in spindle cells that formed a thin rim surrounding clusters of IHBCs, some of which had a small central lumen or were organized in distinct immature bile ducts (Fig. 5). These MSA-positive spindle cells were interpreted to be myofibroblasts surrounding clusters of IHBCs that were differentiating into cholangiocytes and organizing into bile ducts. Hepatocytes, cholangiocytes and myofibroblasts surrounding bile ducts and blood vessels served as internal positive controls and had diffuse intense cytoplasmic immunoreactivity for RFP, CK and MSA, respectively. In livers with oval cell hyperplasia, numerous hepatocytes, cholangiocytes, IHBCs and oval cells were immunoreactive for PCNA (Fig. 3). Rare hepatocytes or cholangiocytes were immunoreactive for PCNA in control livers. Positive PCNA immunoreactivity in the transient amplifying cells of the intestinal crypts served as positive controls. Results of IHC are summarized in Table 3.

### Transmission Electron Microscopy

The oval cells in the liver of fish exposed to DMN exhibited ultrastructural characteristics similar to rodent oval cells or human HPCs (Fig. 6). These fusiform to polygonal cells were located next to or between differentiated or intermediate (immature) hepatocytes. They were consistently located away from sinusoids and, occasionally, contact with BPDEC’s was evident (Fig. 7). The fish oval cells had scant to moderate amounts of organelle-poor cytoplasm and no basal lamina. Few mitochondria and occasional scant endoplasmic reticulum and presumptive lysosomes were present. The adjacent intermediate (immature) hepatocytes exhibited features of hepatocyte differentiation. They had increased amounts of cytoplasm with more numerous mitochondria; increased amounts of glycogen; and exhibited development of rough endoplasmic reticulum. The livers of the MCLR-exposed fish were not evaluated by TEM.

## Discussion

Animal models of human diseases are essential to elucidate molecular mechanisms and develop diagnostic and therapeutic approaches. Detailed knowledge of the biology and tissue response to injury of such models is crucial for selection of appropriate models and

accurate interpretation of study results. In the present study, exposure to MCLR and DMN was performed to induce a hepatic response to injury characterized by prominent proliferation of oval cells. Characterization of this cell population was conducted using histology, single and double IHC, and TEM (DMN exposure only). Use of anti CK AE1/AE3 antibody was selected because this reagent reliably labels cholangiocytes and BPDECs, but not hepatocytes in medaka (Bunton, 1993, 1994; Okihiro and Hinton, 2000). To overcome the lack of a fish hepatocyte marker, a transgenic medaka that expressed an RFP exclusively in mature hepatocytes was used. IHC for actin filaments was performed in order to confirm that the presumptive oval cells were not activated stellate cells or myofibroblasts. The lack of immunoreactivity of stellate cells and myofibroblasts with mammalian α-SMA antibodies necessitated the use of an antibody for MSA that is known to react with SMA in medaka (Bunton, 1995; Hobbie *et al*., 2011).

Exposure to MCLR was performed to induce severe acute hepatic necrosis followed by tissue regeneration. This process was evaluated by histology and IHC with the aim of identifying transient amplifying cell populations derived from the HPCs (Fournie and Courtney, 2002; Fausto and Campbell, 2003; Riehle *et al*., 2011). The range of microscopical regenerative changes observed was similar to that described in other fish species including the hardhead catfish (*Arius felis*), gulf killifish (*Fundulus grandis*) and rainbow trout (Kotak *et al*., 1996; Fournie and Courtney, 2002). In the subset of fish that developed hepatic necrosis and survived long enough to show evidence of a regenerative response, liver regeneration occurred by proliferation of CK-positive oval cells that organized into tubules and resembled human ductular reaction type 3 (Desmet, 2011). Acquisition of hepatocyte morphology at a later time was concomitant with loss of CK immunoreactivity and acquisition of RFP immunoreactivity. These findings are in accordance with studies in people and rats in which oval cell and IHBCs are first positive for CK7/19, but expression is lost as hepatocyte differentiation progresses (Desmet, 2011). Surprisingly, mitotic figures were rare in this transient amplifying oval cell population. However, PCNA IHC confirmed that these cells were actively proliferating.

The medaka livers used for this part of the study were part of MCLR dose range-finding exposures. Interestingly, the liver response to the MCLR dose used in this study was highly variable between fish and its use was not a reliable means of inducing non-lethal hepatic necrosis followed by regeneration. Approximately 80% of the fish did not show any hepatic response to MCLR exposure, while in the remaining 20%, hepatic necrosis was severe and lethal. It is unclear why the fish that survived the phase of acute hepatic necrosis and had histological evidence of hepatic regeneration died 2–4 days after exposure. No histological lesions were observed in other organs.

DMN is a potent carcinogenic hepatotoxin that has been used to induce hepatic fibrosis and neoplasia in a number of fish species, including medaka, as well as in rodents (Jenkins *et al*., 1985; Swenberg *et al*., 1991; Hasegawa *et al*., 1998; Hobbie *et al*., 2011). However, in this study, exposure to DMN was used to induce oval cell hyperplasia (Thoolen *et al*., 2010; Hobbie *et al*., 2011; Van Wettere *et al*., 2012). The subset of DMN-exposed livers that exhibited prominent oval cell hyperplasia was selected and evaluated by IHC and TEM. The CK immunoreactivity and ultrastructural features of the medaka oval cell were consistent

with that reported in mammals (Factor *et al*., 1994; Tan *et al*., 2002; Sobaniec-Lotowska *et al*., 2007; Desmet, 2011). The variable immunoreactivity and occasional double reactivity for CK and RFP of the cells with a histological morphology transitional between oval cells and hepatocytes supported the contention that they were IHBCs (Tan *et al*., 2002; Desmet, 2011). In addition, the observation of RFP-negative IHBCs organizing into distinct ductules was indicative of differentiation towards a biliary epithelial cell phenotype. IHC for MSA proved to be useful in highlighting the IHBCs that were differentiating towards cholangiocytes. A thin rim of MSA-positive spindle cells surrounded small clusters of IHBCs, often with a visible small central lumen as well as immature bile ductules. These spindle cells were likely to be myofibroblasts. A mixture of oval cells, IHBCs, hepatocytes and cholangiocytes were positive for PCNA, suggesting that replication of all cell types occurred during hepatic regeneration after DMN injury. It was expected that most of the proliferating cells would be oval cells and IHBCs, but an estimated similar number of hepatocytes were positive for PCNA. Since PCNA has a long half-life and is also involved in DNA repair, it is possible that some of the immunoreactivity observed was not indicative of active cell division.

In order to provide additional evidence that the oval cells observed on histology were progenitor cells, TEM was performed on the DMN-exposed livers displaying oval cell hyperplasia. The ultrastructural features of the oval cells and IHBCs were similar to those in rodents and man (Factor *et al*., 1994; Sobaniec-Lotowska *et al*., 2007; Hardman *et al*., 2007). The lack of distinguishing features (i.e. cell morphology and type and amount of specific organelles) of the oval cells was supportive of a non-differentiated/stem cell-like state. The observation of larger cells with hepatocyte features, adjacent to oval cells, correlated well with oval cells differentiating towards hepatocytes.

Collectively, results from this study demonstrate that fish oval cells share similar histological and ultrastructural morphology, and immunoreactivity with rodent oval cells and human IHBCs. Moreover, the results support a bipotential lineage of medaka oval cells differentiating towards both hepatocytes and cholangiocytes (Fig. 8). Nonetheless, the results of the study cannot exclude the possibility of dedifferentiation of hepatocytes into proliferating progenitor-like cells. Studies have provided evidence that mature hepatocytes have the ability to dedifferentiate into liver progenitor cells *in vitro*, and also possibly *in vivo* (Braun and Sangren, 2000; Chen *et al*., 2012; Limaye, 2010). However the direct contribution of mature hepatocytes and cholangiocytes to the hepatic progenitor cell pool remains a subject of debate (Malato *et al*., 2011). Cell lineage tracing studies would be one means of investigating this postulate in medaka. Lastly, these results also provide additional evidence of the striking morphological similarities in the hepatic regenerative process between fish and mammals and, thus, further validate the use of small fish models to study the mechanisms of liver reaction to injury.

## Acknowledgments

We are indebted to Drs. J. Renn and C. Winkler, Department of Biological Sciences, National University of Singapore, for providing the founder transgenic medaka for our colony. We are grateful to S. Horton, M. Matmeuller, L. Shewmon and the staff of the Histopathology Laboratory, as well as J. Shipley-Phillips from the Laboratory for Advanced Electron and Light Optical Methods at the NCSU-CVM for their expertise. We also thank

S. Gadi for help with the medaka exposures and maintenance. This work was supported in part by a pilot research grant from the Center for Comparative Medicine and Translational Research at North Carolina State University and a National Institute of Environmental Health Sciences training grant T32-ES007046-31. A. J. Van Wettere is supported by a Ruth L. Kirschstein National Research Service Award T32 RR024394 as part of NCSU's comparative medicine and translational research training program.

## References

Boorman GA, Botts S, Bunton TE, Fournie JW, Harshbarger JC, et al. Diagnostic criteria for degenerative, inflammatory, proliferative non-neoplastic and neoplastic liver lesions in kedaka (*Oryzias latipes*): consensus of a national toxicology program pathology working group. Toxicologic Pathology. 1997; 25:202–210.

Braun KM, Sandgren EP. Cellular origin of regenerating parenchyma in a mouse model of severe hepatic injury. American Journal of Pathology. 2000; 157:561–569. [PubMed: 10934158]

Bunton TE. The immunocytochemistry of cytokeratin in fish tissues. Veterinary Pathology. 1993; 30:418–425. [PubMed: 7505508]

Bunton TE. Intermediate filament reactivity in hyperplastic and neoplastic lesions from medaka (*Oryzias latipes*). Experimental and Toxicologic Pathology. 1994; 46:389–396. [PubMed: 7534529]

Bunton TE. Expression of actin and desmin in experimentally induced hepatic lesions and neoplasms from medaka (*Oryzias latipes*). Carcinogenesis. 1995; 16:1059–1063. [PubMed: 7767965]

Chen Y, Wong PP, Sjeklocha L, Steer CJ, Sahin MB. Mature hepatocytes exhibit unexpected plasticity by direct dedifferentiation into liver progenitor cells in culture. Hepatology. 2012; 55:563–574. [PubMed: 21953633]

Cheng KC, Hinton DE, Mattingly CJ, Planchart A. Aquatic models, genomics and chemical risk management. Comparative Biochemistry and Physiology, Part C: Toxicology and Pharmacology. 2012; 155:169–173.

Couch JA, Courtney LA. N-nitrosodiethylamine-induced hepatocarcinogenesis in estuarine sheepshead minnow (*Cyprinodon variegatus*): neoplasms and related lesions compared with mammalian lesions. Journal of the National Cancer Institute. 1987; 79:297–321. [PubMed: 3474464]

Desmet V. Ductal plates in hepatic ductular reactions. Hypothesis and implications. I. Types of ductular reaction reconsidered. Virchow's Archive. 2011; 458:251–259.

Djediat C, Malécot M, de Luze A, Bernard C, Puiseux-Dao S, et al. Localization of microcystin-LR in medaka fish tissues after cyanotoxin gavage. Toxicon. 2010; 55:531–535. [PubMed: 19837107]

Dykstra, MJ. Manual of Applied Techniques for Biological Electron Microscopy. Plenum Press; New York: 1993.

Evarts RP, Nagy P, Nakatsukasa H, Marsden E, Thorgeirsson SS. In vivo differentiation of rat liver oval cells into hepatocytes. Cancer Research. 1989; 49:1541–1547. [PubMed: 2466557]

Factor VM, Radaeva SA, Thorgeirsson SS. Origin and fate of oval cells in dipin-induced hepatocarcinogenesis in the mouse. American Journal of Pathology. 1994; 145:409–422. [PubMed: 8053498]

Fausto N, Campbell JS. The role of hepatocytes and oval cells in liver regeneration and repopulation. Mechanisms of Development. 2003; 120:117–130. [PubMed: 12490302]

Fournie JW, Courtney LA. Histopathological evidence of regeneration following hepatotoxic effects of the cyanotoxin microcystin-LR in the hardhead catfish and gulf killifish. Journal of Aquatic Animal Health. 2002; 14:273–280.

Hardman RC, Volz DC, Kullman SW, Hinton DE. An in vivo look at vertebrate liver architecture: three-dimensional reconstructions from medaka (*Oryzias latipes*). Anatomical Record. 2007; 290:770–782.

Hasegawa R, Futakuchi M, Mizoguchi Y, Yamaguchi T, Shirai T, et al. Studies of initiation and promotion of carcinogenesis by N-nitroso compounds. Cancer Letters. 1998; 123:185–191. [PubMed: 9489487]

Hinton DE, Couch JA, Teh SJ, Courtney LA. Cytological changes during progression of neoplasia in selected fish species. Aquatic Toxicology. 1988; 11:77–112.

Hinton, DE.; Segner, H.; Au, DWT.; Kullman, SK.; Hardman, RC. Liver Toxicity. In: Di Giulio, RT.; Hinton, DE., editors. The Toxicology of Fishes. CRC Press; Boca Raton: 2008. p. 327-400.

Hobbie KR, Deangelo AB, George MH, Law JM. Neoplastic and non-neoplastic liver lesions induced by dimethylnitrosamine in Japanese medaka fish. Veterinary Pathology. 2011; 49:372–385. [PubMed: 21724976]

Jenkins SA, Grandison A, Baxter JN, Day DW, Taylor I, et al. A dimethylnitrosamine-induced model of cirrhosis and portal hypertension in the rat. Journal of Hepatology. 1985; 1:489–499. [PubMed: 4056351]

Kan NG, Junghans D, Izpisua Belmonte JC. Compensatory growth mechanisms regulated by BMP and FGF signaling mediate liver regeneration in zebrafish after partial hepatectomy. FASEB Journal. 2009; 23:3516–3525. [PubMed: 19546304]

Korzh S, Pan X, Garcia-Lecea M, Winata C, Pan X, et al. Requirement of vasculogenesis and blood circulation in late stages of liver growth in zebrafish. BMC Developmental Biology. 2008; 8:84. [PubMed: 18796162]

Kotak BG, Semalulu S, Fritz DL, Prepas EE, Hrudey SE, et al. Hepatic and renal pathology of intraperitoneally administered microcystin-LR in rainbow trout (*Oncorhynchus mykiss*). Toxicon. 1996; 34:517–525. [PubMed: 8783446]

Limaye PB, Bowen WC, Orr A, Apte UM, Michalopoulos GK. Expression of hepatocytic- and biliary-specific transcription factors in regenerating bile ducts during hepatocyte-to-biliary epithelial cell transdifferentiation. Comparative Hepatology. 2010; 2:9. [PubMed: 21126359]

Malato Y, Naqvi S, Schürmann N, Ng R, Wang B, et al. Fate tracing of mature hepatocytes in mouse liver homeostasis and regeneration. Journal of Clinical Investigation. 2011; 121:4850–4860. [PubMed: 22105172]

Malbrouck C, Kestemont P. Effects of microcystins on fish. Environmental Toxicology and Chemistry. 2006; 25:72–86. [PubMed: 16494227]

McDowell EM, Trump BF. Histologic fixatives suitable for diagnostic light and electron microscopy. Archives of Pathology and Laboratory Medicine. 1976; 100:405–414. [PubMed: 60092]

Mikhail S, He AR. Liver cancer stem cells. International Journal of Hepatology. 2011; 2011:article ID 486954.

Nunez O, Hendricks DJ, Fong TA. Inter-relationships among aflatoxin B1 (AFB1) metabolism, DNA-binding, cytotoxicity, and hepatocarcinogenesis in rainbow trout *Oncorhynchus mykiss*. Diseases of Aquatic Organisms. 1990; 9:15–23.

Oh SH, Witek RP, Bae SH, Zheng D, Jung Y, et al. Bone marrow-derived hepatic oval cells differentiate into hepatocytes in 2-acetylaminofluorene/partial hepatectomy-induced liver regeneration. Gastroenterology. 2007; 132:1077–1078. [PubMed: 17383429]

Okihiro MS, Hinton DE. Partial hepatectomy and bile duct ligation in rainbow trout (*Oncorhynchus mykiss*): histologic, immunohistochemical and enzyme histochemical characterization of hepatic regeneration and biliary hyperplasia. Toxicologic Pathology. 2000; 28:342–356. [PubMed: 10805153]

Ostrander G, Blair J, Stark B, Marley G, Bales W, et al. Long-term primary culture of epithelial cells from rainbow trout (*Oncorhynchus mykiss*) liver. In Vitro Cellular and Developmental Biology: Animal. 1995; 31:367–378. [PubMed: 7543343]

Poss KD. Getting to the heart of regeneration in zebrafish. Seminars in Cell and Developmental Biology. 2007; 18:36–45. [PubMed: 17178459]

Riehle KJ, Dan YY, Campbell JS, Fausto N. New concepts in liver regeneration. Journal of Gastroenterology and Hepatology. 2011; 26:203–212. [PubMed: 21199532]

Roskams TA, Theise ND, Balabaud C, Bhagat G, Bhathal PS, et al. Nomenclature of the finer branches of the biliary tree: canals, ductules, and ductular reactions in human livers. Hepatology. 2004; 39:1739–1745. [PubMed: 15185318]

Sadler KC, Krahn KN, Gaur NA, Ukomadu C. Liver growth in the embryo and during liver regeneration in zebrafish requires the cell cycle regulator, uhrf1. Proceedings of the National Academy of Sciences of the USA. 2007; 104:1570–1575. [PubMed: 17242348]

Sobaniec-Lotowska ME, Lotowska JM, Lebensztejn DM. Ultrastructure of oval cells in children with chronic hepatitis B, with special emphasis on the stage of liver fibrosis: the first pediatric study. World Journal of Gastroenterology. 2007; 13:2918–2922. [PubMed: 17589940]

Swenberg JA, Hoel DG, Magee PN. Mechanistic and statistical insight into the large carcinogenesis bioassays on N-nitrosodiethylamine and N-nitrosodimethylamine. Cancer Research. 1991; 51:6409–6414. [PubMed: 1933905]

Tan J, Hytiroglou P, Wieczorek R, Park YN, Thung SN, et al. Immunohistochemical evidence for hepatic progenitor cells in liver diseases. Liver. 2002; 22:365–373. [PubMed: 12390471]

Thoolen B, Maronpot RR, Harada T, Nyska A, Rousseaux C, et al. Proliferative and nonproliferative lesions of the rat and mouse hepatobiliary system. Toxicologic Pathology. 2010; 38:5S–81S. [PubMed: 21191096]

Van Wettere AJ, Law JM, Hinton DE, Kullman SW. Anchoring hepatic gene expression with development of fibrosis and neoplasia in a toxicant-induced fish model of liver injury. Toxicologic Pathology. 2012 Epub ahead of print, Nov 28.

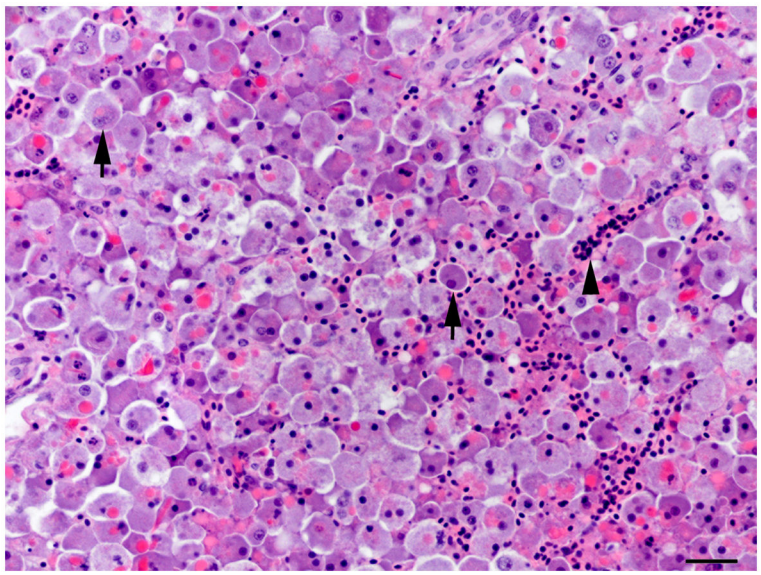

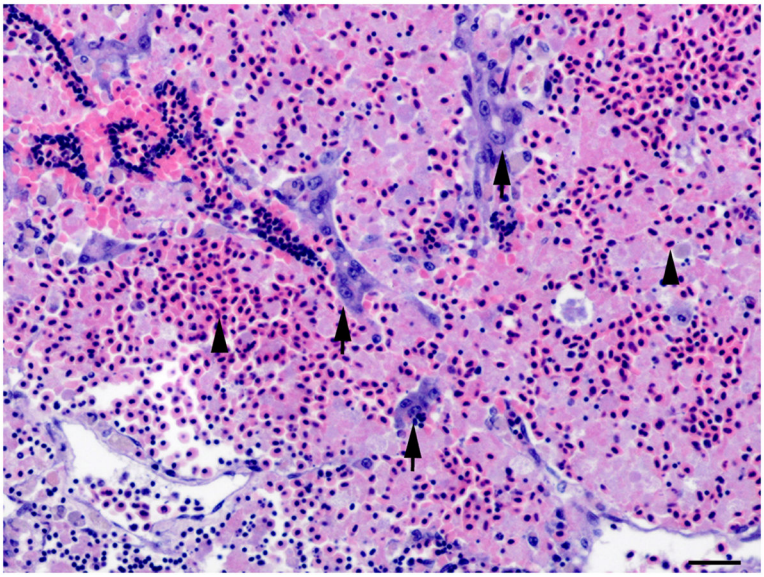

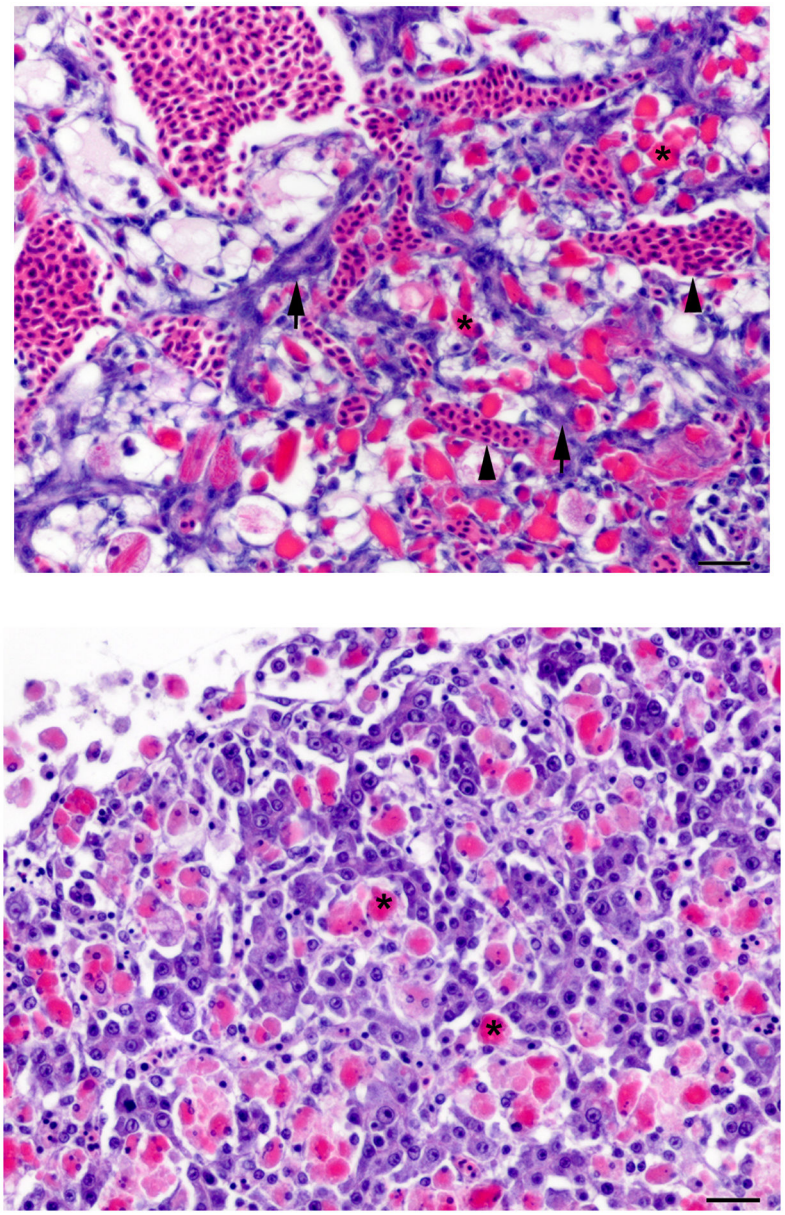

**Fig. 1.**

Histology of the regenerative liver response following microcystin LR (MCLR) exposure. (A) Severe diffuse peracute hepatic necrosis 14 h after MCLR exposure. The hepatic parenchyma is composed of dissociated rounded hepatocytes with pyknotic nuclei (arrow). HE. Bar, 30 μm. (B) Early hepatic regeneration 24 h after MCLR exposure. Basophilic oval cells (arrows) organized in clusters and tubules resembling the human ductular reaction are scattered within the necrotic hepatocellular parenchyma. HE. Bar, 30 μm. (C) Early hepatic regeneration 36 h after MCLR exposure. Tubules formed by basophilic oval cells often have a visible slit-like lumen (arrows) and are interconnected. Between the oval cells, numerous macrophages infiltrate the parenchyma (asterisks) and are filled with bright red cell debris due to ingestion of the hepatocytic RFP. HE. Bar, 30 μm. (D) Hepatic regeneration 48 h post

exposure. The hepatic parenchyma is mostly composed of intermediate hepatobiliary cells and the infiltrate of macrophages (asterisk) is reduced. HE. Bar, 30 μm. Arrowheads in the figures indicate red blood cells.

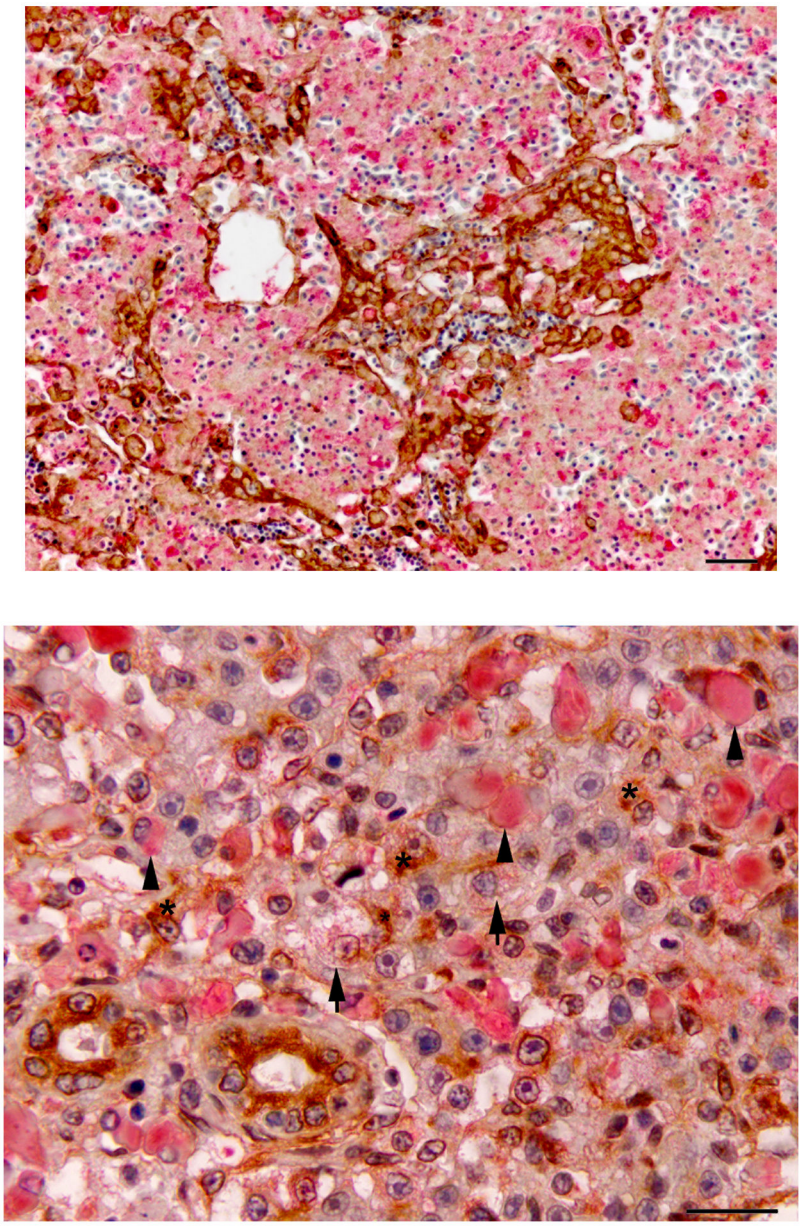

**Fig. 2.**

Hepatic regeneration following microcystin LR (MCLR) exposure; double immunolabelling for CK AE1/AE3 and red fluorescent protein (RFP). (A) Early hepatic regeneration 24 h after MCLR exposure. Oval cells (arrow) are strongly positive for CK (brown). Surrounding cell debris is variably immunoreactive for RFP (red). Double IHC for CK and RFP, haematoxylin counterstain. Bar, 30μm. (B) Hepatic regeneration 96 h post exposure to MCLR. The hepatic parenchyma is composed of intermediate hepatobiliary cells that are occasionally weakly positive for RFP (arrow). A small number of CK-positive oval cells are still present (asterisk). Cholangiocytes are also positive for CK. Macrophages display variable cytoplasmic expression of RFP (arrowheads). Double IHC for CK and RFP, haematoxylin counterstain. Bar, 20 μm.

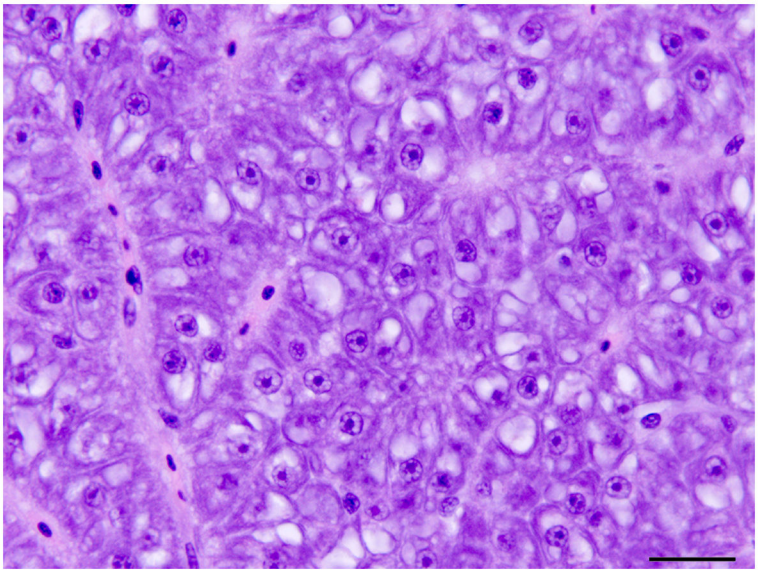

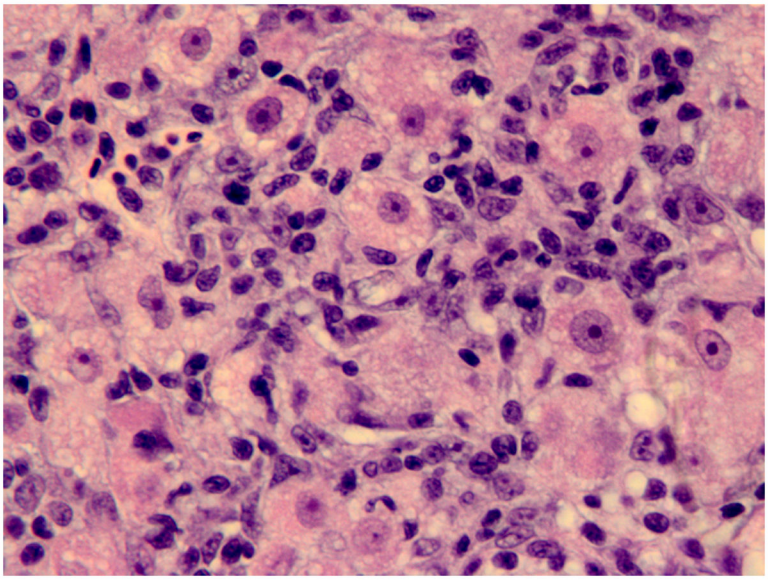

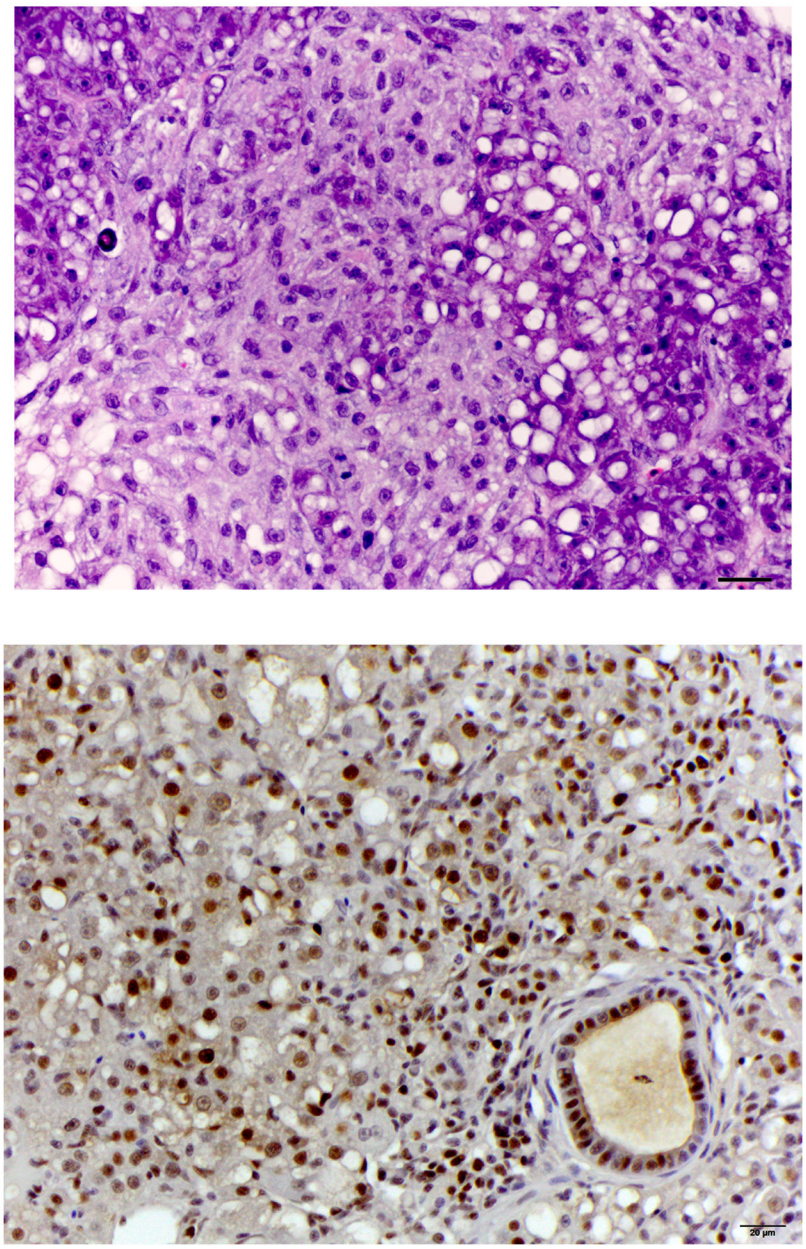


**Fig. 3.**

Histology of control liver and liver with oval cell hyperplasia. (A) Normal female medaka liver. HE. Bar, 20 µm. (B) Oval cell hyperplasia characterized by proliferation of small cells with a hyperchromatic elongated nuclei that separate the hepatocyte tubules and sometimes surround individual hepatocytes. HE. Bar, 20 µm. (C) Focus of oval cells differentiating towards hepatocytes. HE. Bar, 20 µm. (D) Liver, oval cell hyperplasia after DMN exposure. Oval cells, hepatocytes and cholangiocytes demonstrate nuclear immunoreactivity for PCNA of variable intensity. IHC. Bar, 50 µm.

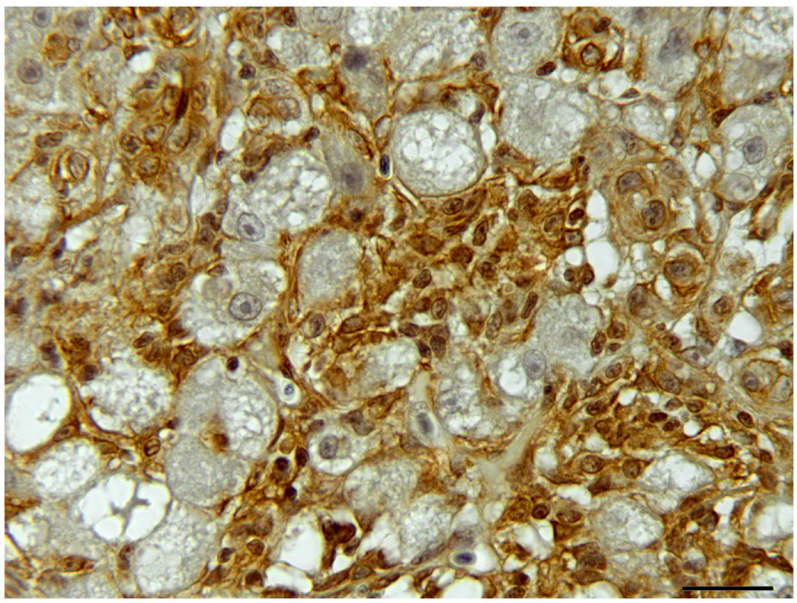

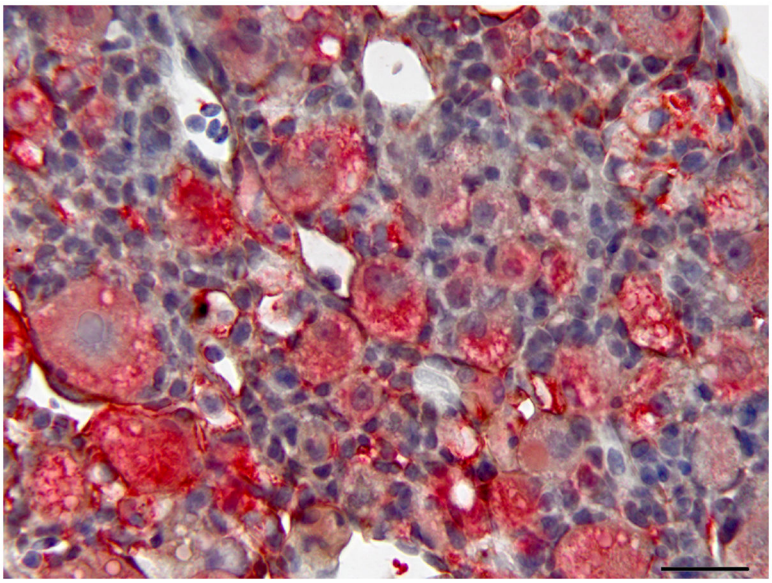

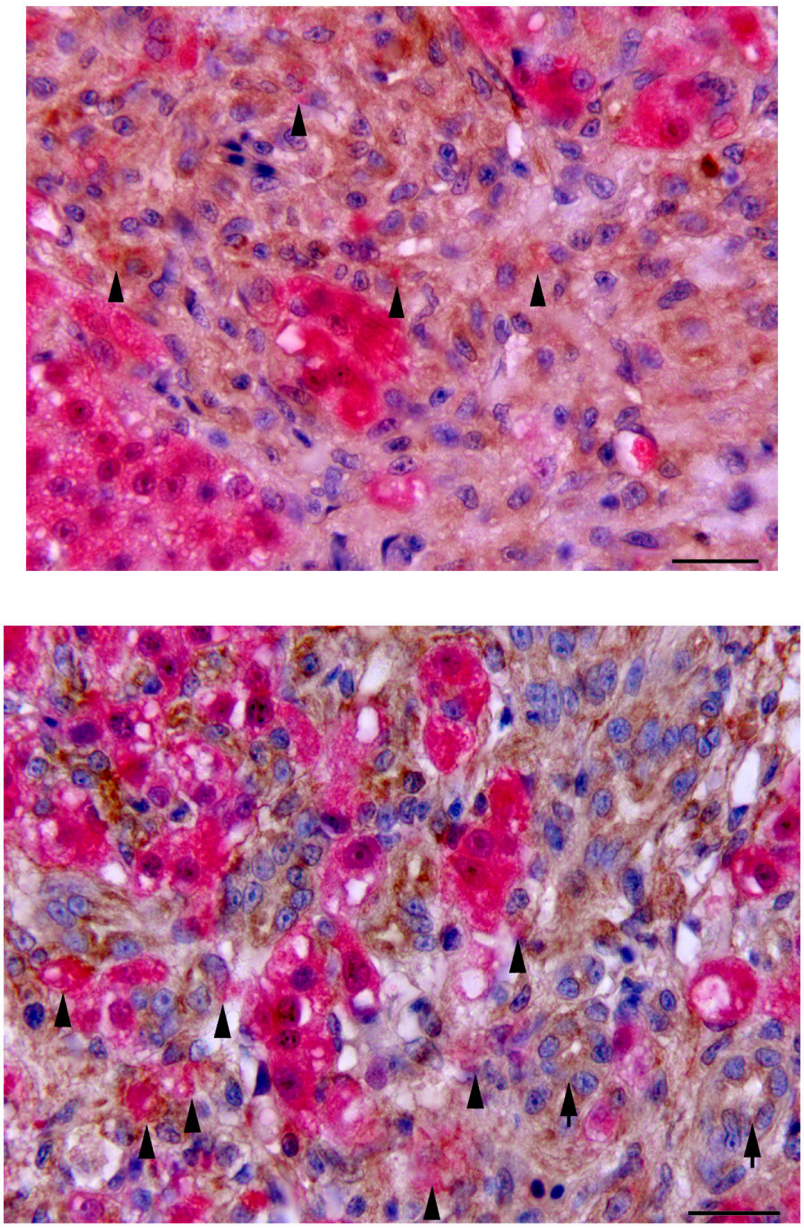

**Fig. 4.**

Single and double immunolabelling for CK AE1/AE3 and RFP in regenerating liver. (A) Liver, oval cell hyperplasia following DMN exposure. Oval cells are positive for CK (brown). CK AE1/AE3 IHC. Bar, 20 μm. (B–D) Oval cells differentiating into hepatocytes admixed with hepatocytes after DMN exposure. (B) Hepatocytes are positive for RFP (red). Weak to occasionally moderate immunoreactivity for RFP is present in the intermediate hepatobiliary cells. IHC. Bar, 20 μm. (C and D) Oval cells positive for CK (brown) and hepatocytes positive for RFP (red) are admixed with intermediate hepatobiliary cells positive for RFP and CK (arrowheads). CK-positive oval cells form immature bile ducts (arrows). Double IHC for CK and RFP. Bar, 20 μm.

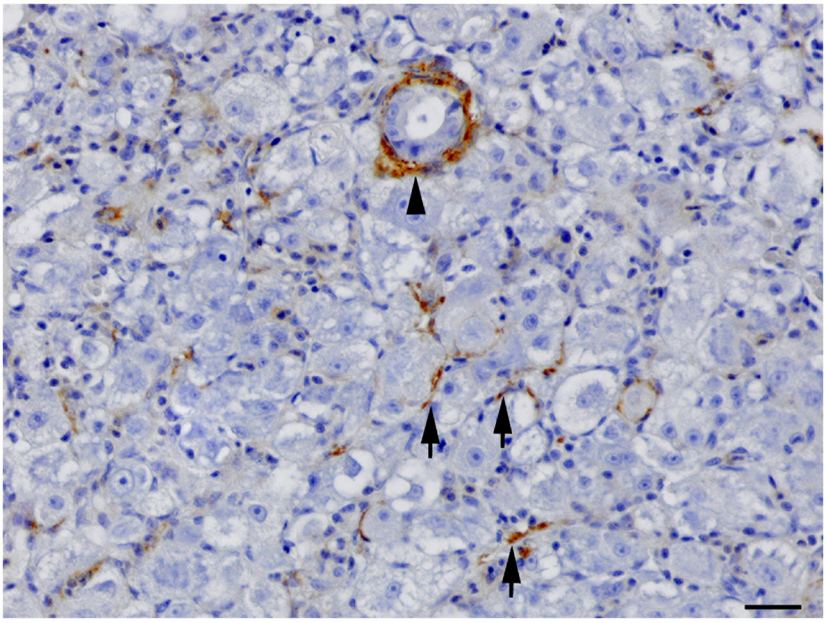

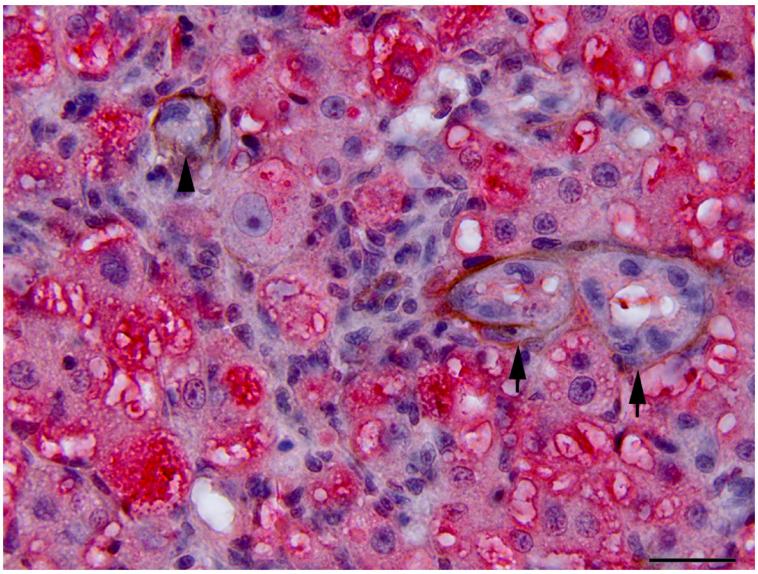

**Fig. 5.**

Single immunolabelling for muscle specific actin (MSA) and double immunolabelling for MSA and red fluorescent protein (RFP) in regenerating liver. (A) Oval cell hyperplasia after DMN exposure. Activated stellate cells (arrows) and myofibroblasts (arrow heads) are positive for MSA. IHC. Bar, 50 μm. (B) Oval cells and intermediate hepatobiliary cells admixed with hepatocytes after DMN exposure. Two immature bile ducts formed by RFP-negative intermediate hepatobiliary cells are surrounded by a thin rim of MSA-positive cells (arrows). Other RFP-negative intermediate hepatobiliary cells are surrounded by a rim of MSA-positive cells, but no duct lumen is present yet (arrowhead). Double IHC for MSA and RFP. Bar, 20 μm.

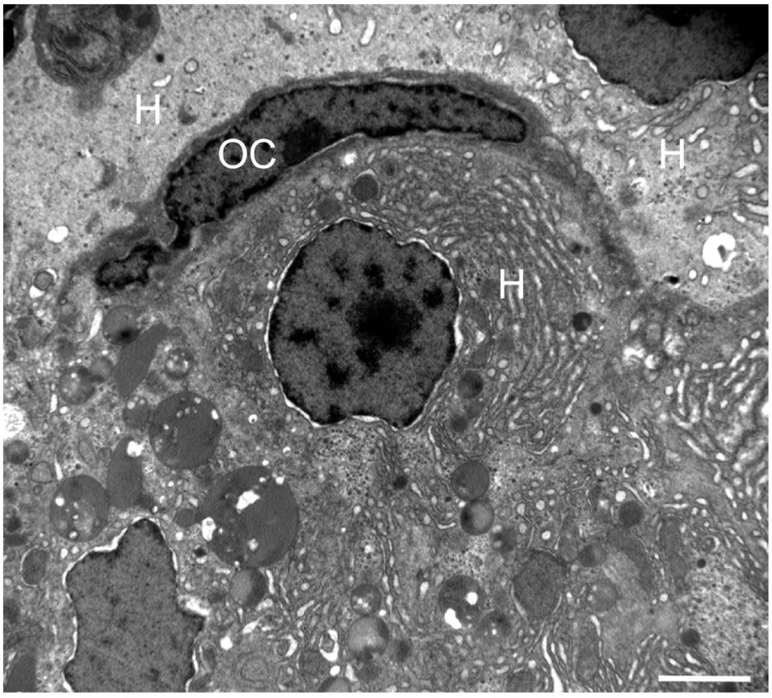


**Fig. 6.**

Transmission electron microscopy of the liver of a DMN-exposed medaka with oval cell hyperplasia. An oval cell (OC) is adjacent to three hepatocytes (H). Note the organelle-poor cytoplasm and lack of distinguishing morphological features of the OC. See Fig. 3b for the histological correlate. Bar, 2 μm.

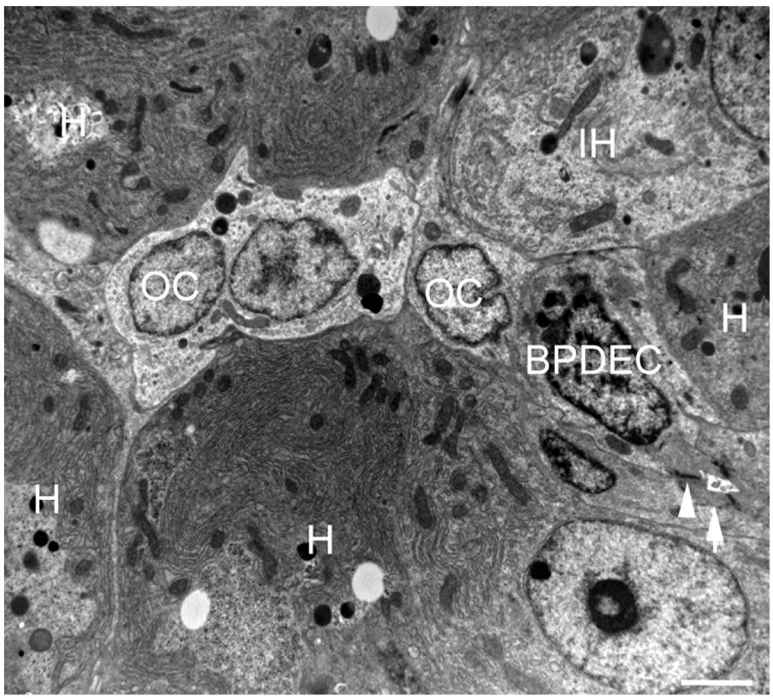


**Fig. 7.**

Transmission electron microscopy of the liver of a DMN-exposed medaka with oval cell hyperplasia. A row of oval cells (OC) is located between hepatocytes (H) and in contact with a bile preductular epithelial cell (BPDEC) and a cell showing features of hepatocyte differentiation (immature hepatocytes [IH]) including increased cell volume, increased nuclear size, greater number of mitochondria, increased glycogen and development of rough endoplasmic reticulum. A biliary canaliculus formed by a BPDEC and hepatocytes is visible (arrow). Junctional complexes are indicated by arrowheads. Bar, 2 μm.

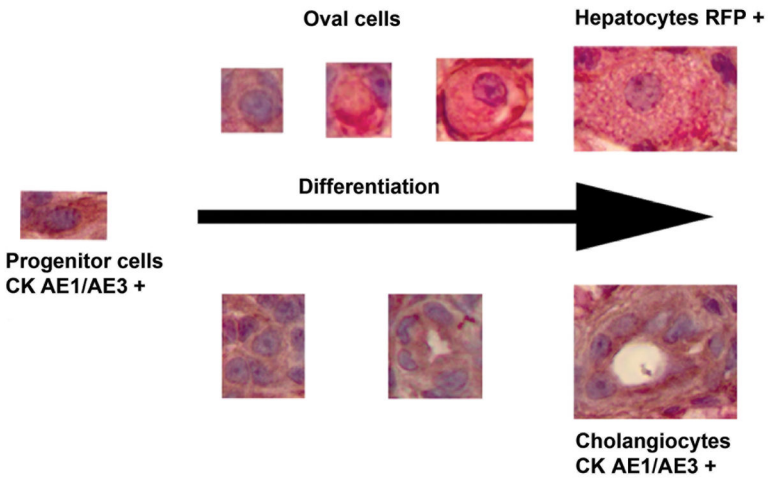


**Fig. 8.**

Proposed piscine hepatic progenitor cell differentiation processes towards hepatocytes and cholangiocytes through oval cells.

**Table 1**

Immunohistochemical markers used in this study

| Name | Company | Type | Antibody dilution | Function | Reactivity |
|---|---|---|---|---|---|
| Cytokeratin AE1/AE3* | BioGenex Laboratories, San Ramon, California, USA. Catalogue # AM0751-5M | Mouse monoclonal | Prediluted antibody | Recognizes high- and low-molecular-weight cytokeratins | Bile duct epithelium, BPDECs and oval cells |
| Muscle Specific actin (MSA) | BioGenex Laboratories, Catalogue # MU090-UC | Mouse monoclonal (HHF35), IgG1 | 1 in 100 | Reacts with 42 kD protein specific for actin in skeletal, cardiac, and smooth muscle | Periductal smooth muscle cells, activated stellate cells |
| Proliferating Cell Nuclear Antigen (PCNA) | BioGenex Laboratories, Catalogue # MU252-UC | Mouse monoclonal (PC10), IgG2a | 1 in 250 | Reacts with a 36 kD non-histone nuclear protein auxiliary of DNA polymerrases δ and ε enzymes necessary for DNA synthesis | Cell in the G1, S and G2/ Mphases of cell cycle |
| Red fluorescent protein | Abcam, Cambridge, Massachusetts , USA. Catalogue # ab34771 | Rabbit polyclonal | 1 in 500 | Reacts with RFP protein full length amino acid sequence (234aa) from the mushroom polyp coral *Discosoma* | Transgenic hepatocytes expressing the RFP |

* AE1 recognizes CK 10, 14, 15, 16 and 19; AE3 recognizes CK 1, 2, 3, 4, 5, 6 and 8

**Table 2**

Histopathological findings after microcystin LR exposure

| Time post exposure (hours) | 100 µg/kg (*n* = 21) | | 250 µg/kg (*n* = 27) | | 500 µg/kg (*n* = 12) | |
|---|---|---|---|---|---|---|
| | **Died** | **Killed** | **Died** | **Killed** | **Died** | **Killed** |
| 14 | | | HN: 2<br>HNR: 1 | | HN: 2 | |
| 24 | NL: 5<br>HNR: 1 | HNR: 2 | HN: 2<br>HNR: 1 | | | |
| 36 | | | HNR: 1 | | HN: 1<br>HNR: 2 | |
| 48 | NL: 2<br>HNR: 1 | | HN: 1<br>HNR: 2 | NL: 2 | | |
| 72 | | | HR: 1<br>U:1 | | HNR: 1 | |
| 96 | | NL: 2 | HR: 2 | | | |
| 144 | | | | NL: 6 | | NL: 4 |
| 192 | | NL: 8 | | NL: 4<br>FHR: 1 | | NL: 2 |

U, unknown due to marked autolysis; NL, no lesion; HN, hepatic necrosis; HNR, hepatic necrosis with regeneration (diffuse hepatic necrosis with multifocal tubules and/or aggregates of basophilic oval cells); HR, hepatic regeneration (liver composed of oval cells, immature hepatocytes and numerous individual and aggregate of macrophages); FHR, focus of hepatic regeneration (normal liver with a focal area of oval cells and immature hepatocytes and moderate number of macrophages filled with cell debris).

**Table 3**

Summary of Immunohistochemical Expression Analysis

| Marker | Hepatocyte | Cholangiocyte | Oval cell | Oval cell with hepatocyte features | Myofibroblast and activated stellate cell |
|---|---|---|---|---|---|
| Cytokeratin AE1/AE3 | − | +++ | +++ | (+) | − |
| RFP | +++ | − | − | (+) | − |
| MSA | − | − | − | − | +++ |
| PCNA (DMN exposure) | ++ | ++ | + | ++ | − |
| PCNA (MCLR exposure) | + | + | +++ | + | − |

RFP, red fluorescent protein; MSA, muscle specific actin; PCNA, proliferating cell nuclear antigen; DMN, dimethylnitrosamine; MCLR, microcystin LR.

Immunoreactivity scoring: − absent; (+) variable and mild; + mild; ++ moderate; +++ marked.